Scientific Research Publishing

Open Journal of Applied Sciences, 2025, 15(9), 2556-2567
https://www.scirp.org/journal/ojapps
ISSN Online: 2165-3925
ISSN Print: 2165-3917

Characteristic Study of Intense Storms: Case of the Intense Storms of November 6, 1997, August 17, 2001, and January 7, 2015

Karim Guibula[1,2*], Abidina Diabate[1,3], Rassiratou Kindo[1], Frédéric Ouattara[1,4]

[1]Laboratory of Analytical Chemistry, Space Physics and Energy (L@CAPSE), Norbert Zongo University, Koudougou, Burkina Faso
[2]Physics Department, Virtual University of Burkina Faso, Ouagadougou, Burkina Faso
[3]Physics Department, Nazi Boni University, Bobo-Dioulasso, Burkina Faso
[4]Physics Department, Norbert Zongo University, Koudougou, Burkina Faso
Email: *kariguib92@gmail.com

How to cite this paper: Guibula, K., Diabate, A., Kindo, R. and Ouattara, F. (2025) Characteristic Study of Intense Storms: Case of the Intense Storms of November 6, 1997, August 17, 2001, and January 7, 2015. *Open Journal of Applied Sciences*, **15**, 2556-2567.
https://doi.org/10.4236/ojapps.2025.159170

Received: April 5, 2025
Accepted: July 25, 2025
Published: September 3, 2025

Abstract

The characteristics of three intense geomagnetic storms and the influence of solar phases on their intensity were studied. The extreme values of the Dst and AE indices and solar wind parameters (V_{sw}, P_{sw}, B_z, E_y, nP) were used to characterize the storm intensities. The three storms were selected during the solar ascending, maximum, and descending phases, respectively, and with almost identical minimum Dst values. The results show that storm of August 17, 2001, occurring at solar maximum with a prolonged (~10 h) and well-structured south-facing Bz (Bz_{south}), is the most intense. Storm of November 6, 1997, occurring during the ascending phase and characterized by a prolonged (~12 h) but less structured Bz_{south}, and storm of January 7, 2015, occurring during the descending phase and characterized by a well-structured but less prolonged (~5 h) Bz_{south}, are the least intense. It is also observed that intense storms occurring at different solar phases do not have the same characteristics or intensity. These results confirm the importance of solar phases as well as that of the Bz component of the interplanetary magnetic field (IMF), in particular its structure in CMEs and the duration of its southern polarity, in determining the intensity of geomagnetic storms.

Keywords

Geomagnetic Storms, Intense Storms, Bz Component, Geomagnetic Indices, Solar Wind

1. Introduction

Geomagnetic storms are disturbances of the Earth's magnetic field, caused by solar and interplanetary events such as coronal mass ejections (CMEs), fast solar winds, and corotating interaction regions [1] [2]. They are often considered signatures of the dynamics of the Sun-Earth relationship [3].

Geomagnetic storms disrupt terrestrial and space technologies [4]-[6]. Indeed, they affect satellite technologies and disrupt communications systems [7]-[9], radio signals and GPS, space missions, geophysical exploration, power grids, and many other technologies.

There are many studies on geomagnetic storms. Among these, there are studies on 1) the origin of geomagnetic storms [10]-[13], 2) their impact on the terrestrial environment [14]-[16], 3) their occurrence as a function of solar cycles and phases [2] [3] [17]-[20], 4) their classification from indices [1] [6] [11] [21] [22], 5) their relationships to solar wind parameters [23]-[25] and many other topics.

For example, [1] and [10] showed that at Earth, most intense geomagnetic storms are caused by southerly interplanetary magnetic fields (IMFs), carried by a high-speed solar wind. [1] later pointed out that the main causes of geomagnetic storms on Earth are strong dawn-dusk electric fields, accompanied by southerly IMFs near Earth for a sufficiently long duration. [12] studied the solar sources of geomagnetic storms during solar cycle 24. He concluded that the weak geomagnetic activity during cycle 24 is related to the weak dawn-dusk electric field of the solar wind. This author also concludes that the relatively slow CMEs contributed to the geomagnetic storms during cycle 24. [3] studying the occurrence of geomagnetic storms as a function of seasons and time during solar cycles 21-24, observed a higher probability of occurrence of large storms around 21-8 UT during the equinoxes. [20] also studied the occurrence of geomagnetic storms during solar cycles 23 and 24. They found that weak and moderate storms, caused by fast solar winds, are more prevalent in the descending phase of the solar cycle, while strong storms, which are caused by coronal mass ejections (CMEs), are more frequent at solar maximum and then in the descending phase. To classify geomagnetic storms, [11] defined criteria that were taken up and adopted by [26] and [27]. According to these criteria, four classes of geomagnetic storms are distinguished, namely, 1) major storms defined by $Kp_{max} \geq 8$ and $Kp \geq 6$ lasting at least 3 hours during a 24-hour period, 2) large storms defined by $7 \leq Kp_{max} \leq 7+$ and $Kp \geq 6$ lasting at least 3 hours during a 24-hour period; 3) medium storms which include all other cases with $Kp_{max} \geq 6-$ and 4) weak storms characterized by $5- \leq Kp_{max} \leq 5+$. [1], identified three classes of geomagnetic storms according to the minimum values of Dst; namely 1) intense storm ($Dst \geq -100$ nT), 2) moderate storms ($-100 \leq Dst \leq -50$ nT) and weak storms ($-50 \leq Dst \leq -30$ nT). Later, [28] extended this classification to five classes by distinguishing, 1) weak storms ($-50 \leq Dst \leq -30$ nT); 2) moderate storms ($-100 \leq Dst \leq -50$ nT), 3) strong storms ($-200 \leq Dst \leq -100$ nT), 4) severe storms ($-350 \leq Dst \leq -200$ nT) and 5) major storms > -350 nT. [25] analyzed the correlation between geomagnetic storm in-

tensity and solar wind parameters from 1996 to 2023. They found that storm intensity is correlated with the peak values and/or time integral values of the southward interplanetary magnetic field (IMF Bs), twilight electric field (Ey), Akasofu function (ε), and dynamic pressure (P_{sw}) to varying degrees.

The occurrence of geomagnetic storms as a function of solar phases has been widely studied. However, the influence of solar phases on the characteristics of geomagnetic storms is poorly addressed. Thus, to understand the influence of solar phases on the intensity of geomagnetic storms, this study analyzes the characteristics of intense storms (Dst < −100 nT) recorded during different solar phases.

2. Data and Method

In this study, hourly OMNIWEB values of Dst and AE indices, as well as the B_z, Ey, V_{sw}, and P_{sw} parameters, were used to characterize storm intensity. In addition, the Rz index was used to define the solar phases for the years studied. All these indices and parameters are available on the OMNIWEB website at: https://omniweb.gsfc.nasa.gov/form/dx1.html.

SSC dates were used to identify the onset of storms. These dates are available at: https://isgi.unistra.fr/data_download.php.

The three storms studied are intense storms selected on the basis of the Dst index and the criterion defined by [1]. With these criteria we select intense storms having almost the same min Dst and belonging to different solar phases. The Rz values and the criterion defined by [20] made it possible to identify the solar phases of the years of occurrence of the storms considered. **Table 1** gives the dates of occurrence of the three storms and their position in the solar cycle.

Table 1. Dates of appearance of the three storms and the corresponding solar phases.

Storms	Date of occurrence	Corresponding solar phase
Storm 1	06/11/1997	Ascending phase
Storm 2	17/08/2001	Maximum phase
Storm 3	07/01/2015	Descending phase

The extreme values of the AE, Dst indices and the parameters Bz, Ey, V_{sw} and P_{sw} were used to characterize the intensity of storm [24]. The variations of Bz during the main phase of storm allow to characterize its structure in the IMF. Indeed, according to [29], Bz variations are the magnetic signature of the internal structure of the IMF. Thus, a smooth and continuous variation of Bz indicates a well-organized internal structure while abrupt or disordered variations of Bz may signal a disturbed or incomplete structure. The polarities of the Bz allow to identify its orientation. Thus, a positive/negative Bz is a Bz with a North/South orientation [30]. The limits of the phases of a storm were identified on the basis of the SSC and the hourly variations of the Dst index. Thus, **Figure 1** presents the limits of the phases of the three storms studied.

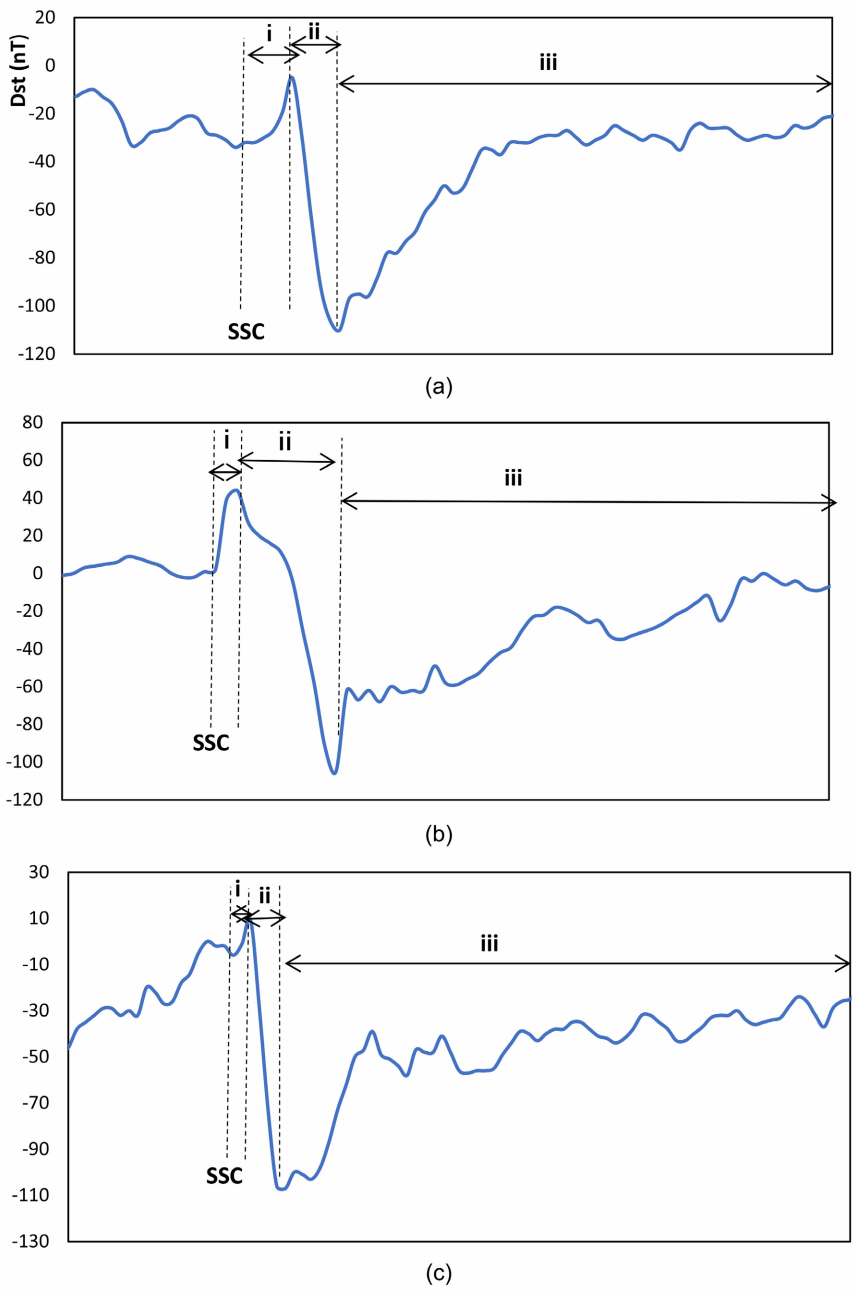

Figure 1. Phases of the storms studied. Panel (a) Storm 1; Panel (b) Storm 2; Panel (c) Storm 3; i: Initial phase; ii: Main phase; iii: Recovery phase.

To observe the evolution of the characteristic parameters of the storms studied, we considered one day before the storm, the day of the storm and two days after the storm to plot the profiles.

3. Results and Analyses

Figures 2-4 present the variations in geomagnetic indices (AE, Dst), solar wind parameters (B_z, V_{sw}, nP, E_y), and magnetospheric parameters (P_{sw}) during the storms of November 6, 1997, August 17, 2001, and January 7, 2015, respectively.

These storms occurred during an ascending phase, a solar maximum, and a descending phase of the sun, respectively. All graphs were plotted over a period of four (04) days.

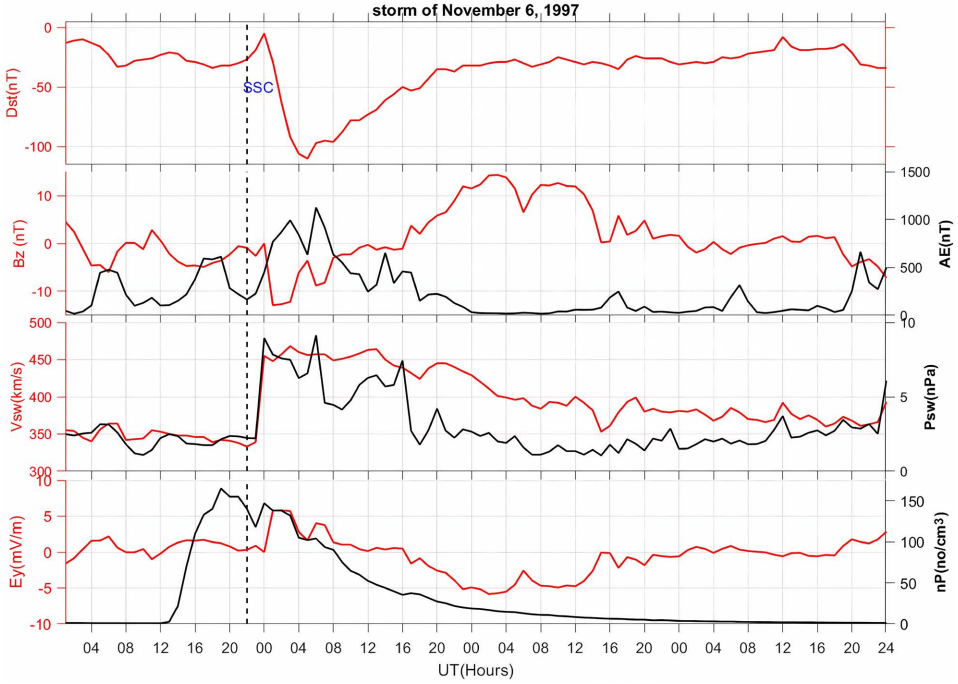

Figure 2. Variations of geomagnetic indices (AE, Dst), solar wind parameters (Bz, V_{sw}, nP, Ey) and magnetospheric parameter (P_{sw}) during Storm of November 6, 1997.

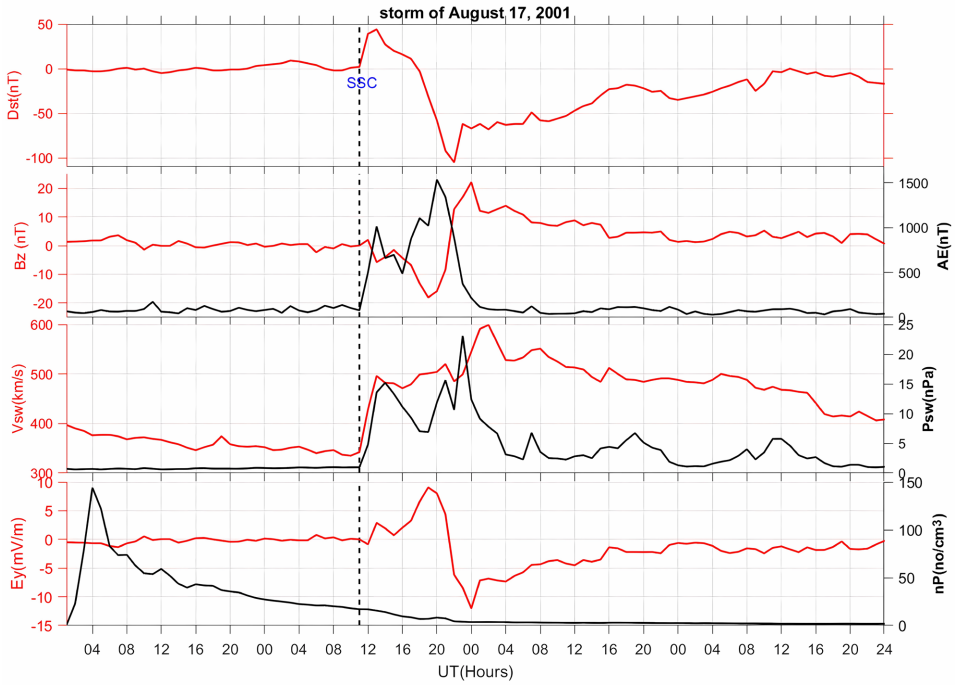

Figure 3. Variations of geomagnetic indices (AE, Dst), solar wind parameters (Bz, V_{sw}, nP, Ey) and magnetospheric parameter (P_{sw}) during storm of August 17, 2001.

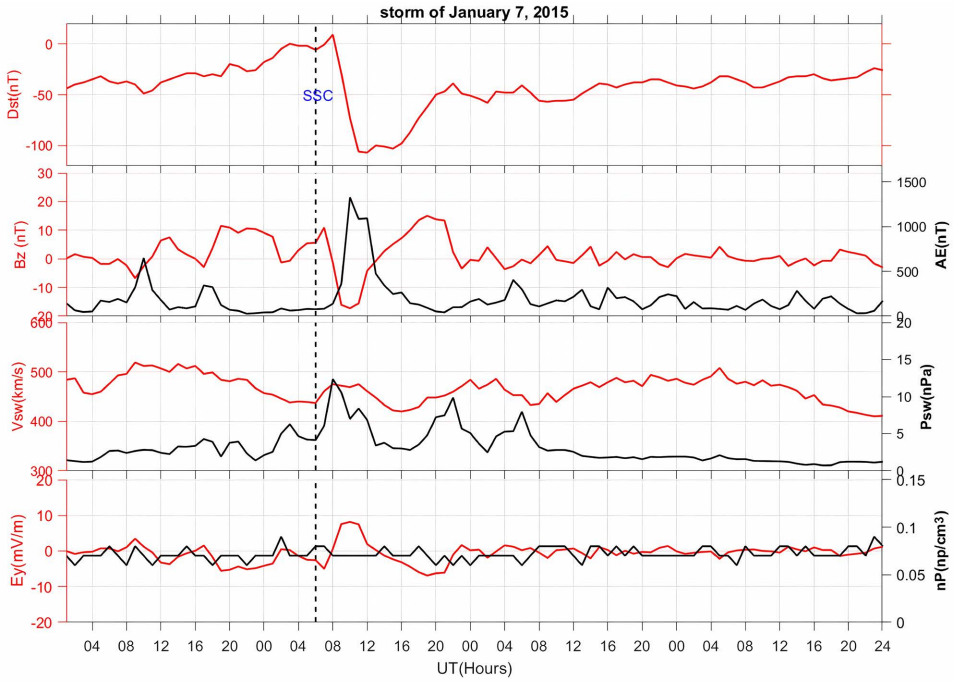

Figure 4. Variations of geomagnetic indices (AE, Dst), solar wind parameters (Bz, V_{sw}, nP, Ey) and magnetospheric parameter (P_{sw}) during storm of January 7, 2015.

3.1. Storm of November 6, 1997

During the initial phase (2200 - 0000 UT of day 1), the Dst index increases from −10 to −5 nT, while the Bz index remains practically low around 0 nT. From the SSC, the auroral activity (AE) increases, the pressure (P_{sw}) and the speed (V_{sw}) of the solar wind increase by 3 - 9 nPa and 350 - 440 km/s respectively. The Ey parameter remains practically constant around 0 mV/m. The particle density (Proton flux > 30 MeV) initially decreases after the SSC and then shows a peak (~140 no/cm^3) at the end of the initial phase.

During the main phase (0000 - 0500 UT of day 2), a drop in the Dst index to ~−110 nT is observed. A prolonged period of negative values of the Bz component is also observed. This period consists of a brief descent phase (0000 - 0100 UT of day 2) and a long, fluctuating ascent phase (0100 - 1200 UT of day 2); Bz_{min} ~ −15 nT is reached during the main phase. There is also a fluctuation in the intensities of auroral activity (AE: 800 - 1200 nT) and the electric field (Ey: 0 - 5 mV/m).

3.2. Storm of August 17, 2001

The initial phase of the storm (1100 - 1300 UT of day 2) is characterized by an increase in Dst of 0 - 49 nT; Bz remains stable around 0 nT between 1100 - 1200 UT of day 2 before decreasing from 0 to −5 nT between 1200 - 1300 UT of day 2. AE, Vsw and Psw increase rapidly from 10 - 950 nT, 330 - 500 km/s and 1 - 10 nPa respectively. Ey remains stable between 1100 - 1200 UT of day 2 and then increases slightly from 0 - 3 mV/m. The nP parameter is not perturbed.

The main phase, which lasted from 1300 - 2100 UT of day 2, is marked by a

gradual drop in the Dst index to −105 nT and a prolonged period of negative values of the Bz component (~10 h). This period, consisting of fairly regular periods of descent and rise of the Bz, indicates a well-structured Bz in the IMF. Bz_{min} = −20 nT reached around 1900 UT of day 2. The main phase is also characterized by the appearance of remarkable peaks of auroral activity (1000 nT, 1500 nT) respectively at the beginning and end of the phase; a solar wind at almost stable speed (500 km/s) with a dynamic pressure fluctuating between 9 - 20 nPa. There is also a strong fluctuation of Ey (−11 and 150 mV/m) and a stable trend in the number of particles (Proton flux > 30 MeV).

3.3. Storm of January 7, 2015

During the initial phase (0600 - 0800 UT of day 2), the Dst index increases slightly (0 - 5 nT); the Bz index fluctuates with a North orientation; the AE index remains constant around 0 nT; the solar wind speed (V_{sw}) increases slightly by 450 - 460 km/s while the dynamic pressure increases strongly by 5 - 14 nPa; the Ey parameter starts to increase from 0500 UT while the particle number (Proton flux > 30 MeV) keeps a stable trend.

The main phase (0700 - 1300 UT of day 2) is characterized by a sharp drop in the Dst index of up to −107 nT; a relatively short-lived South Bz component (08 - 1300 UT) and a Bz_{min} of −20 nT reached at 1000 UT. This brief drop is consistent with a maximum of the AE index between 1000 - 1200 nT. The solar wind speed is moderately high between 500 and 600 km/s, the dynamic pressure decreases by 10 - 5 nPa. The Ey parameter fluctuates between 0 - 12 mV/m but the particle density (Proton flux > 30 MeV) maintains a stable trend around ~0.08 particles/cm^3.

4. Discussion

The three geomagnetic storms (storm 1, storm 2, and storm 3), although all intense, exhibit distinct characteristics related to their position in the solar cycle and the nature of the interplanetary disturbances that triggered them. This diversity is well consistent with the findings of [31], who distinguished between storms caused by coronal mass ejections (CMEs) and those due to high-speed streams from coronal holes (HSSs).

Storm 1 is typical of a storm caused by a CME occurring during a solar upswing phase. We observe a strong persistent negative Bz component (~ −15 nT) over 04 hours, a minimum Dst value close to −110 nT, and an Ey energy > 5 mV/m, corresponding well to an efficient coupling between the solar wind and the magnetosphere. These extremes appear during the main phase, except for the dynamic pressure and particle density which peak at the time of the SSC. This event illustrates a storm caused by a slow CME. According to [1], such a configuration (prolonged southern Bz + Ey > 5 mV/m) is sufficient to cause a moderate energy transfer inducing an intense storm, even in the upswing phase. The simultaneous presence of high particle densities and high dynamic pressure reinforces the compres-

sion of the magnetopause, as confirmed by [32]. This situation well illustrates the classic scenario described by [33] where a slow CME with a strong and stable southerly magnetic field can produce a significant thunderstorm.

Storm 2 is the most intense of the three (Dst ~ −105 nT). It reflects maximum solar activity, with a very strongly negative Bz field (Bzmin = −20 nT) over ~10 hours; which is much greater than the negative Bz extension of the first storm (storm 1); an extreme Ey (>10 mV/m) and a fast solar wind (>500 km/s). It is therefore a fast and violent CME. According to [34], these conditions favor major auroral disturbances, which is here confirmed by extreme values of the AE index (>1500 nT). The high interplanetary electric field induces a massive magnetospheric energy transfer, in accordance with the model of [35]. This configuration is typical of major geomagnetic storms associated with fast CMEs, as shown by [11] and [31]. It illustrates the impact of a structured interplanetary field on the intensity of a storm.

Compared to the first storm (storm 1), the intensity of this one reflects a fast, highly structured CME with a prolonged southern Bz field. The energy transfer to the magnetosphere is maximal, explaining the extreme values of the geomagnetic and auroral indices.

Storm 3 is less intense (Dst ~ −107 nT), which could be due to a less durable southern Bz component and a more moderate Ey (~8 mV/m) thus limiting the magnetosphere-solar wind coupling. The CME at the origin of this storm is probably less organized or oriented in a way less favorable to the coupling. In addition, the auroral activity is intense but over a short period (AE peak ~ 1300 nT at around 1000 UT).

Table 2 summarizes the extreme values of the parameters and indices used to characterize the intensity of the three geomagnetic storms.

Table 2. Extreme values of the characteristic quantities of the three geomagnetic storms.

	Geomagnetic index		Solar wind parameters			
	Min Dst (nT)	Max AE (nT)	Min Bz (nT)	Max Ey (mV/m)	Peak Vsw (km/s)	Peak Psw (nPa)
Storm of November 6, 1997	−110	1125	−15	5.8	468	7.6
Storm of August 17, 2001	−105	1536	−20	12.04	599	23.06
Storm of January 7, 2015	−107	1327	−17.3	8.16	475	8.39

Analyzing the three (3) storms, we note that storm 2, which occurred at solar maximum, is the most intense. It is distinguished by a prolonged (~10 h), well-structured and strongly negative (−20 nT) southern Bz component, a high Ey electric field (~10 mV/m), a fast solar wind (>500 km/s), strong compression on the magnetosphere (>20 nPa), and strong auroral electrojet activity (AE > 1500 nT). Storm 1, which occurred during the ascending solar phase, is a relatively less intense storm than storm 2. It is characterized by a prolonged (~12 h), strongly neg-

ative (~−15 nT) southern Bz but less structured than the previous one. The extreme values of the characteristic parameters and indices of this storm (storm 1) are lower than those of storm 2 (AE = 1125 nT; Ey = 5.8 mV/m; V_{sw} = 468 km/s; Psw = 7.6 nPa). Storm 3, which occurred during the descending phase, is the least intense. It is characterized by a well-structured and strongly negative South Bz component (−17.3 nT) but less prolonged compared to the other two (~5 h); a relatively intense auroral electrojet activity (AE = 1327 nT) over a short duration (~4 h); a weak fluctuation of the Ey field (−1 to 8.16 mV/m), a solar wind speed and a dynamic pressure relatively almost identical to those of storm 1 (475 km/s −8.39 nPa).

The results of these case studies may not apply to all solar cycles. To this end, a larger statistical study involving several solar cycles and several geomagnetic storms could lead to a good generalization of the results.

5. Conclusion

The geomagnetic storms studied exhibit strong variability in intensity, linked to the phase of the solar cycle. The interplanetary magnetic field Bz, its duration in southerly polarity, the electric field Ey, and the dynamic pressure of the solar wind are the main factors influencing storm intensity. The importance of prolonged southerly Bz plus high Ey can cause strong magnetosphere-solar wind coupling. The Dst and AE indices provide a coherent interpretation of storm evolution and its ionospheric impacts. These results confirm the importance of solar phases as well as that of the Bz component of the interplanetary magnetic field (IMF), particularly its structure in CMEs and the duration of its southerly polarity, in determining the intensity of geomagnetic storms.

Conflicts of Interest

The authors declare no conflicts of interest regarding the publication of this paper.

References

[1] Gonzalez, W.D., Joselyn, J.A., Kamide, Y., Kroehl, H.W., Rostoker, G., Tsurutani, B.T., *et al.* (1994) What Is a Geomagnetic Storm? *Journal of Geophysical Research*: *Space Physics*, **99**, 5771-5792. https://doi.org/10.1029/93ja02867

[2] Mishra, W., Sahani, P.S., Khuntia, S. and Chakrabarty, D. (2024) Distribution and Recovery Phase of Geomagnetic Storms during Solar Cycles 23 and 24. *Monthly Notices of the Royal Astronomical Society*, **530**, 3171-3182. https://doi.org/10.1093/mnras/stae1045

[3] Audu, M.O. and Okeke, F.N. (2024) Statistical Analysis and Characterisation of Geomagnetic Storm Occurrence and Its Dependent on Solar Cycle, Season, and Time during Solar Cycles 21-24. *World Scientific News*, **197**, 73-87.

[4] Reyes, P.I., Pinto, V.A. and Moya, P.S. (2021) Geomagnetic Storm Occurrence and Their Relation with Solar Cycle Phases. *Space Weather*, **19**, e2021SW002766. https://doi.org/10.1029/2021sw002766

[5] Oladipo, B.W., Adamu, O.M., Adebiyi, J.L. and Ikubanni, S.O. (2018) Correlation

between Sunspot Number and Geomagnetic Storm. *Equity Journal of Science and Technology*, **5**, 157-161. https://eprints.lmu.edu.ng/2326/1/14-1549897199.pdf

[6] Wu, C., Liou, K., Lepping, R.P., Hutting, L., Plunkett, S., Howard, R.A., *et al.* (2016) The First Super Geomagnetic Storm of Solar Cycle 24: "The St. Patrick's Day Event (17 March 2015)". *Earth, Planets and Space*, **68**, Article No. 151. https://doi.org/10.1186/s40623-016-0525-y

[7] Chapman, S.C., Horne, R.B. and Watkins, N.W. (2020) Using the Aa Index over the Last 14 Solar Cycles to Characterize Extreme Geomagnetic Activity. *Geophysical Research Letters*, **47**, e2019GL086524. https://doi.org/10.1029/2019gl086524

[8] Wrenn, G.L. (2009) Chronology of 'killer' Electrons: Solar Cycles 22 and 23. *Journal of Atmospheric and Solar-Terrestrial Physics*, **71**, 1210-1218. https://doi.org/10.1016/j.jastp.2008.08.002

[9] Wrenn, G.L., Rodgers, D.J. and Ryden, K.A. (2002) A Solar Cycle of Spacecraft Anomalies Due to Internal Charging. *Annales Geophysicae*, **20**, 953-956. https://doi.org/10.5194/angeo-20-953-2002

[10] Gonzalez, W.D. and Tsurutani, B.T. (1987) Criteria of Interplanetary Parameters Causing Intense Magnetic Storms ($D_{st} < -100$ nT). *Planetary and Space Science*, **35**, 1101-1109. https://doi.org/10.1016/0032-0633(87)90015-8

[11] Gosling, J.T., McComas, D.J., Phillips, J.L. and Bame, S.J. (1991) Geomagnetic Activity Associated with Earth Passage of Interplanetary Shock Disturbances and Coronal Mass Ejections. *Journal of Geophysical Research*: *Space Physics*, **96**, 7831-7839. https://doi.org/10.1029/91ja00316

[12] Watari, S. (2017) Geomagnetic Storms of Cycle 24 and Their Solar Sources. *Earth, Planets and Space*, **69**, Article No. 70. https://doi.org/10.1186/s40623-017-0653-z

[13] Bothmer, V. and Schwenn, R. (1995) The Interplanetary and Solar Causes of Major Geomagnetic Storms. *Journal of Geomagnetism and Geoelectricity*, **47**, 1127-1132. https://doi.org/10.5636/jgg.47.1127

[14] Chiaha, S.O., Ugonabo, O.J. and Okpala, K.C. (2019) A Study on the Effects of Solar Wind and Interplanetary Magnetic Field on Geomagnetic H-Component during Geomagnetic Storms. *International Journal of Physical Sciences*, **14**, 38-44. https://doi.org/10.5897/ijps2018.4772

[15] Astafyeva, E., Yasyukevich, Y.V., Maletckii, B., Oinats, A., Vesnin, A., Yasyukevich, A.S., *et al.* (2022) Ionospheric Disturbances and Irregularities during the 25-26 August 2018 Geomagnetic Storm. *Journal of Geophysical Research*: *Space Physics*, **127**, e2021JA029843. https://doi.org/10.1029/2021ja029843

[16] Astafyeva, E., Zakharenkova, I., Hozumi, K., Alken, P., Coïsson, P., Hairston, M.R., *et al.* (2018) Study of the Equatorial and Low-Latitude Electrodynamic and Ionospheric Disturbances during the 22-23 June 2015 Geomagnetic Storm Using Ground-based and Spaceborne Techniques. *Journal of Geophysical Research*: *Space Physics*, **123**, 2424-2440. https://doi.org/10.1002/2017ja024981

[17] Kilpua, E.K.J., Olspert, N., Grigorievskiy, A., Käpylä, M.J., Tanskanen, E.I., Miyahara, H., *et al.* (2015) Statistical Study of Strong and Extreme Geomagnetic Disturbances and Solar Cycle Characteristics. *The Astrophysical Journal*, **806**, Article No. 272. https://doi.org/10.1088/0004-637x/806/2/272

[18] Patowary, R. and Bhuyan, K. (2012) A Study of Seasonal Variation of Geomagnetic Activity. *Research Journal of Physical and Applied Sciences*, **2**, 1-11.

[19] Katus, R.M., Liemohn, M.W., Ionides, E.L., Ilie, R., Welling, D. and Sarno-Smith, L.K. (2015) Statistical Analysis of the Geomagnetic Response to Different Solar Wind

Drivers and the Dependence on Storm Intensity. *Journal of Geophysical Research*: *Space Physics*, **120**, 310-327. https://doi.org/10.1002/2014ja020712

[20] Sawadogo, Y., Koala, S. and Zerbo, J.L. (2022) Factors of Geomagnetic Storms during the Solar Cycles 23 and 24: A Comparative Statistical Study. *Scientific Research and Essays*, **17**, 46-56. https://doi.org/10.5897/sre2022.6751

[21] Parashar, K.K., Rathore, B.S., Kaushik, S.C., Kapil, P. and Gupta, D.C. (2011) Classification and Study of Geomagnetic Storms during Year 1996-2010. *International Journal of Pure and Applied Physics*, **7**, 199-202.

[22] Mansilla, G.A. (2013) Solar Cycle and Seasonal Distribution of Geomagnetic Storms with Sudden Commencement. *Earth Science Research*, **3**, 50-55. https://doi.org/10.5539/esr.v3n1p50

[23] Kleimenova, N.G. and Kozyreva, O.V. (2014) Global Pi3 Geomagnetic Pulsations as a Response of Large Variations in the Solar Wind and IMF during the Magnetic Storm of August 5, 2011. *Geomagnetism and Aeronomy*, **54**, 195-202. https://doi.org/10.1134/s001679321402011x

[24] Subedi, A., Adhikari, B. and Mishra, R.K. (2017) Variation of Solar Wind Parameters during Intense Geomagnetic Storms. *Himalayan Physics*, **6-7**, 80-85. https://doi.org/10.3126/hj.v6i0.18366

[25] Sun, X., Hu, Y., Zhima, Z., Duan, S., Lv, F. and Shen, X. (2024) Joint Observations of the Large-Scale ULF Wave Activity from Space to Ground Associated with the Solar Wind Dynamic Pressure Enhancement. *Science China Technological Sciences*, **67**, 2215-2229. https://doi.org/10.1007/s11431-023-2663-6

[26] Richardson, I.G., Cane, H.V. and Cliver, E.W. (2002) Sources of Geomagnetic Activity during Nearly Three Solar Cycles (1972-2000). *Journal of Geophysical Research*: *Space Physics*, **107**, SSH 8-1-SSH 8-13. https://doi.org/10.1029/2001ja000504

[27] Richardson, I.G. and Cane, H.V. (2012) Solar Wind Drivers of Geomagnetic Storms during More than Four Solar Cycles. *Journal of Space Weather and Space Climate*, **2**, A01. https://doi.org/10.1051/swsc/2012001

[28] Loewe, C.A. and Prölss, G.W. (1997) Classification and Mean Behavior of Magnetic Storms. *Journal of Geophysical Research*: *Space Physics*, **102**, 14209-14213. https://doi.org/10.1029/96ja04020

[29] Wu, C. and Lepping, R.P. (2006) Solar Cycle Effect on Geomagnetic Storms Caused by Interplanetary Magnetic Clouds. *Annales Geophysicae*, **24**, 3383-3389. https://doi.org/10.5194/angeo-24-3383-2006

[30] Moon, G. (2011) Variation of Magnetic Field (B_y, B_z) Polarity and Statistical Analysis of Solar Wind Parameters during the Magnetic Storm Period. *Journal of Astronomy and Space Sciences*, **28**, 123-132. https://doi.org/10.5140/jass.2011.28.2.123

[31] Zhang, J., Richardson, I.G., Webb, D.F., Gopalswamy, N., Huttunen, E., Kasper, J.C., *et al.* (2007) Solar and Interplanetary Sources of Major Geomagnetic Storms ($Dst \leq -100$ nT) during 1996-2005. *Journal of Geophysical Research*: *Space Physics*, **112**, A10102. https://doi.org/10.1029/2007ja012321

[32] Russell, C.T., Ginskey, M., Petrinec, S. and Le, G. (1992) The Effect of Solar Wind Dynamic Pressure Changes on Low and Mid-Latitude Magnetic Records. *Geophysical Research Letters*, **19**, 1227-1230. https://doi.org/10.1029/92gl01161

[33] Tsurutani, B.T. and Gonzalez, W.D. (1997) The Interplanetary Causes of Magnetic Storms: A Review. In: Huang, L.J., Eds., *Geophysical Monograph Series*, American Geophysical Union, 77-89. https://doi.org/10.1029/gm098p0077

[34] Kamide, Y., Yokoyama, N., Gonzalez, W., Tsurutani, B.T., Daglis, I.A., Brekke, A., *et*

al. (1998) Two-Step Development of Geomagnetic Storms. *Journal of Geophysical Research*: *Space Physics*, **103**, 6917-6921. https://doi.org/10.1029/97ja03337

[35] Burton, R.K., McPherron, R.L. and Russell, C.T. (1975) An Empirical Relationship between Interplanetary Conditions and *DST*. *Journal of Geophysical Research*, **80**, 4204-4214. https://doi.org/10.1029/ja080i031p04204